Journal of Power Sources 185 (2008) 1598–1604

Contents lists available at ScienceDirect

Journal of Power Sources

journal homepage: www.elsevier.com/locate/jpowsour

# Hydrogen in thin Pd-based layers deposited on reticulated vitreous carbon—A new system for electrochemical capacitors

M. Łukaszewski [a], A. Żurowski [a], A. Czerwiński [a,b,*]

[a] Warsaw University, Department of Chemistry, Pasteura 1, 02-093 Warsaw, Poland
[b] Industrial Chemistry Research Institute, Rydygiera 8, 01-793 Warsaw, Poland

ARTICLE INFO

*Article history:*
Received 13 May 2008
Received in revised form 10 July 2008
Accepted 3 August 2008
Available online 13 August 2008

*Keywords:*
Reticulated vitreous carbon (RVC)
Palladium
Pd–Rh alloys
Hydrogen absorption
Supercapacitors

ABSTRACT

Reticulated vitreous carbon (RVC) has been used as a matrix for electrodeposition of thin layers of Pd and Pd-rich Pd–Rh alloys. It was found that RVC substrate does not affect qualitatively hydrogen absorption behavior of Pd-based deposits. Similarly to thin Pd or Pd alloy layers deposited on Au wires, the α–β phase transition controls the overall rate of hydrogen absorption and desorption into/from Pd-based/RVC electrodes. The possibility of the application of these materials as phase charging–discharging systems was investigated. The values of specific pseudocapacitance, specific power and specific energy were comparable with those for supercapacitors utilizing various redox reactions.



## 1. Introduction

Hydrogen–metal systems have been investigated for almost 150 years [1], in both fundamental and application aspects. They have been successfully applied as: (i) catalysts in hydrogenation reactions, (ii) source of hydrogen of high purity by thermal decomposition of hydrides, (iii) reacting substances in synthesis of transition metal alloys, (iv) neutron moderators in nuclear power engineering, (v) membranes for hydrogen purification and hydrogen isotopes separation, (vi) anodes in nickel-hydride batteries (Ni-MH) and (vii) hydrogen storage materials.

Pd is historically the first metal known to absorb hydrogen [1]. It rapidly absorbs large amounts of hydrogen from the gas phase as well as from the electrolytes [2]. When hydrogen absorption is performed from the gas phase, $H_2$ molecules dissociate into atoms chemisorbed on the Pd surface and then diffuse into the bulk of the metal. When hydrogen absorption is performed electrochemically, after application of a suitable potential value H atoms are generated on the electrode from hydrogen-containing species present in the solution, e.g. $H^+$ ions in acidic solutions. Absorbed hydrogen occupies octahedral voids in Pd crystal lattice [3] forming a non-stoichiometric compound, $PdH_x$. It was established using the methods of neutron diffraction and NMR that hydrogen is present inside Pd not in the molecular form but most probably in the form of protons [4]. Hydrogen in Pd can exist in two phases [1]: α-phase (i.e. solid solution of hydrogen in Pd), for which at room temperature the atomic ratio between hydrogen and Pd (H/Pd) is below ca. 0.03–0.05, and β-phase (i.e. non-stoichiometric Pd hydride), which corresponds to H/Pd ratio above ca. 0.6. Pd crystal lattice expands during hydrogen absorption by more than 3% in the β-phase in comparison with pure metal [5,6].

Pd alloying with other metals modifies the absorption properties of the system with respect to pure Pd [1,3,5–11]. These modifications result from the alteration of the electronic structure (electronic effect) and crystal lattice dimensions (geometric effect), as well as from changes in elastic properties caused by the alloying process. Among Pd alloys the Pd–Rh system seems to be particularly interesting, since for a low Rh content the amount of absorbed hydrogen is equal to or even greater than in pure Pd [12–14]. It is an exception to the rule that Pd mixing with a non-absorbing element (such as Rh) weakens the hydrogen absorption capacity [1,3,7–11].

It should be mentioned that Pd and its alloys with other noble metals are especially attractive and convenient for electrochemical experiments due to the fact that hydrogen absorption can be realized at room temperature without corrosion of the electrode material [15]. Moreover, the use of a thin (of the order of microns) metal layer deposited on a hydrogen-neutral conducting matrix, e.g. Au or carbon material, has created new possibilities for electrochemical studies of hydrogen-absorbing materials [16–24]. Such

* Corresponding author at: Warsaw University, Department of Chemistry, Pasteura 1, 02-093 Warsaw, Poland. Tel.: +48 22 8220211; fax: +48 22 8225996.
*E-mail address:* aczerw@chem.uw.edu.pl (A. Czerwiński).

0378-7753/$ – see front matter © 2008 Elsevier B.V. All rights reserved.
doi:10.1016/j.jpowsour.2008.08.002

an approach allows for the limitation and control of the amount of absorbed hydrogen. These electrodes are called 'limited volume electrodes' (LVEs).

Since hydrogen can be electrochemically inserted into and extracted from Pd-based electrodes, such materials can be treated as phase charging–discharging systems for electrochemical capacitors. These devices usually utilize the capacitance of electrical double layer of various carbon materials or pseudocapacitance connected with reversible redox processes like insertion of atomic species into the crystal structure of bulk solid electrodes, e.g. conducting polymers or transition metal oxides (mostly $RuO_2$) [25–28]. Due to high currents generated during hydrogen uptake and removal as well as good practical reversibility of these processes, thin Pd-based layers electrolytically loaded with hydrogen seem particularly promising for that purpose.

In our study reticulated vitreous carbon (RVC) has been chosen as a matrix for deposition of thin Pd and Pd–Rh layers. RVC is an inexpensive and chemically inert carbon material characterized by an open pore structure and highly developed surface [29–31]. It has been widely applied as an electrode material, including the use as a substrate for deposition of various metals, such as Au [32,33], Pt [34,35], Rh [35], Pd [19,20,36–38], Ru [39], Ni [40], Pb [41,42] and alloys, e.g. Pt–Rh [35,38] and Pd–Rh [38]. Due to its unique properties RVC is attractive for electrochemical studies and can be regarded as an electrode matrix applicable to energy storage systems [30,31,43–48].

In this work we extend our earlier studies on hydrogen absorption in Pd-based deposits on RVC [19,20,38]. We have examined the influence of RVC substrate on hydrogen absorption behavior. We show the characteristic of these materials as phase charging–discharging systems that could be applied in electrochemical capacitors.

## 2. Experimental

All experiments were performed at room temperature in 0.5 M $H_2SO_4$ solutions deoxygenated using an Ar stream. A $Hg|Hg_2SO_4|0.5\ M\ H_2SO_4$ was used as the reference electrode. A Pt gauze was used as the auxiliary electrode. All potentials are recalculated with respect to the SHE.

Reticulated vitreous carbon (RVC) of 20 ppi porosity grade, made by ERG, Material and Aerospace Corporation, has been used as a matrix for electrodeposition of Pd and Pd–Rh alloys. The electrodes were in the form of blocks of a volume of 0.2–0.5 $cm^3$. Since density of this material is 0.048 g $cm^{-3}$ and surface-to-volume ratio for 20 ppi is 14 $cm^2$ $cm^{-3}$ [30], the electrodes used were typically of mass of 10–20 mg and surface area of 3–7 $cm^2$.

RVC substrate was always degreased with acetone followed by keeping in boiling water for ca. 20 min. Pd and Pd–Rh alloys were deposited on RVC at constant potential from baths containing $PdCl_2$ and $RhCl_3$ in HCl [38]. Additionally, RVC electroplated with Au layer was also employed as the substrate for the deposits. The thickness of the deposits as calculated from deposition charge was in the range 0.6–1.0 μm, which corresponded to 0.7–1.3 mg $cm^{-2}$ of deposited metal per surface area. For comparison, the deposits on Au wires (99.9%, 0.5 mm diameter) were also used.

The morphology of the surfaces was examined by a LEO 435VP scanning electron microscope (SEM). Bulk composition of Pd–Rh alloys was determined in electrochemical experiment from the potential of α–β phase transition, which was found to depend linearly on bulk Pd content [49]. All alloy compositions given in this work are expressed in atomic percentages.

At the beginning of experiments each electrode was cycled continuously through the potential region of hydrogen adsorption and absorption until a steady-state voltammogram was obtained. This procedure took several tens of absorption/desorption cycles and was applied in order to avoid effects of ageing during further hydrogen insertion/removal.

## 3. Results and discussion

Fig. 1 shows SEM images of bare RVC matrix and RVC electroplated with a thin Pd layer. It is visible that tight deposits fully covering the substrate were obtained. SEM inspections at high magnifications revealed that the crystalline size of the deposited metal varied from tens to hundreds of nanometers.

General electrochemical behavior of the samples was examined by cyclic voltammetry. Fig. 2 presents cyclic voltammogram recorded for Pd/RVC electrode in the full potential range. The well known features are visible connected with hydrogen adsorption/absorption/desorption (currents below ca. 0.3 V), double layer charging (0.3–0.6 V) and surface oxide formation/reduction (above ca. 0.6 V). The CV curve is very similar to those known for thin Pd deposits on other kinds of substrates, like Au [19–22,24]. One should note the voltammogram course in hydrogen region. Typically of Pd-LVEs, hydrogen can be absorbed and totally removed during a single voltammetric reduction–oxidation cycle, and after hydrogen removal current drops to values connected only with double layer charging unless potential is sufficiently high for electrode surface oxidation [16]. For comparison CV curve for bare RVC is shown. It is

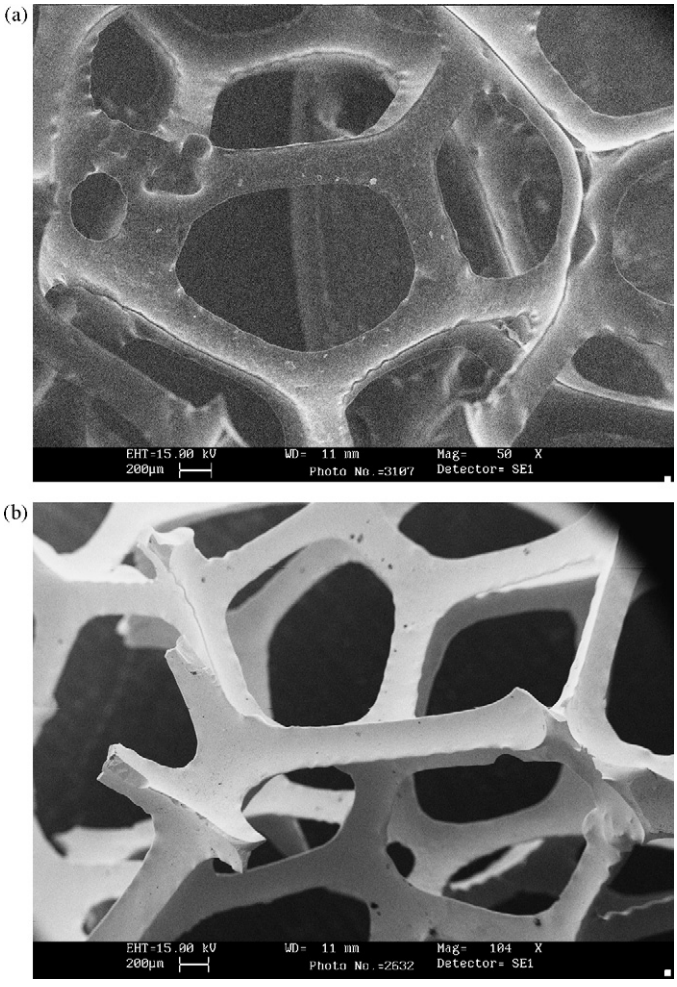


**Fig. 1.** SEM images of bare RVC (a) and Pd deposit on RVC (b).

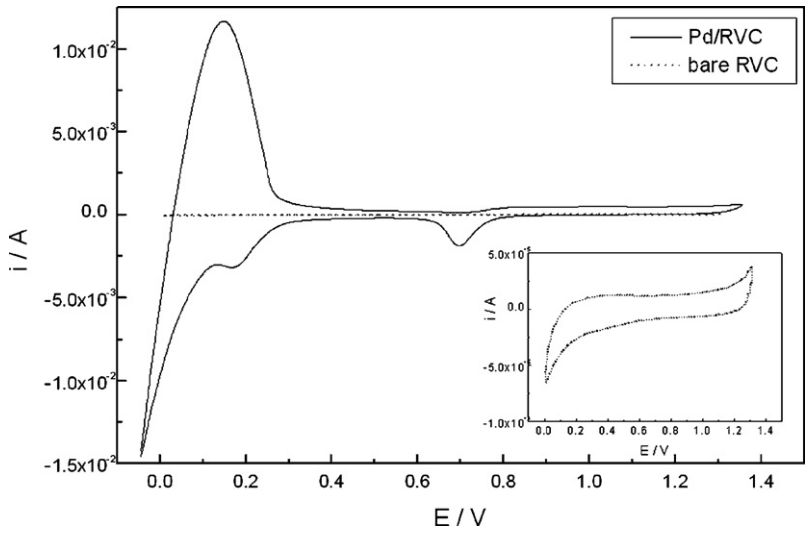


**Fig. 2.** Cyclic voltammogram for Pd/RVC electrode in 0.5 M $H_2SO_4$ in the full potential range (−0.05 to 1.35 V), scan rate 0.01 V $s^{-1}$. Data for bare RVC are shown for comparison.

clearly visible that this material is not electrochemically active in the potential range applied.

Fig. 3 presents the dependence of the amount of electrosorbed hydrogen (expressed as hydrogen-to-metal ratio) on the electrode potential, obtained in two ways [14,50]: (a) from the charge of chronoamperometric oxidation (at 0.45 V) of hydrogen electrosorbed at a given potential, (b) from the difference of charges corresponding to the amount of hydrogen electrosorbed at −0.05 V and hydrogen oxidized at a given potential. Procedures (a) shows the influence of potential on the amount of hydrogen loaded during absorption, while procedure (b) yields the potential dependence of the amount of hydrogen remaining in the electrode during desorption.

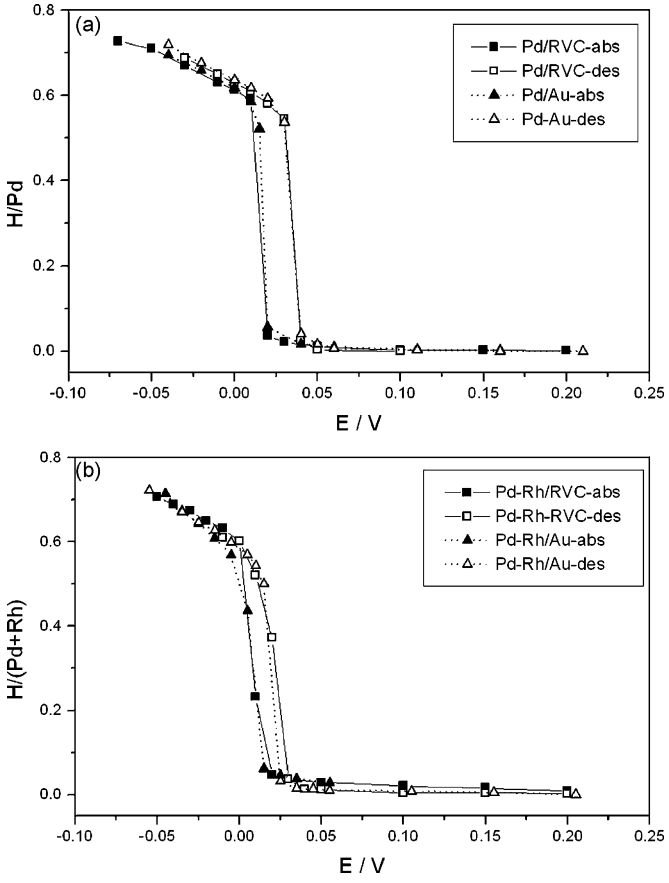


**Fig. 3.** Hydrogen absorption capacities vs. potential for absorption (solid symbols) and desorption (open symbols) obtained in chronoamperometric experiments in 0.5 M $H_2SO_4$: (a) Pd, (b) 97% Pd–Rh alloy.

These plots exhibit three characteristics potential regions corresponding to various forms of hydrogen present in the system. Initially, the amount of electrosorbed hydrogen rises slowly with decreasing potential, which mirrors the processes of hydrogen adsorption and α-phase formation. Then a sharp increase in the absorption capacity is observed in a narrow potential range, which can be attributed to the α–β phase transition. For lower potentials absorbed hydrogen exists as the hydrogen-rich β-phase.

As can be seen in Fig. 3, the plots obtained in procedures (a) and (b) are similar in the regions of α and β phases but differ in the phase transition region, which for absorption series (solid symbols) is placed at a lower potential than for the desorption series (open symbols). This behavior corresponds to the effect of hysteresis well known for gas-phase measurements, where hydrogen pressure connected with the α–β equilibrium during absorption course is higher than during desorption course [1,7,51,52]. It is visible that the potential ranges of α–β and β–α transitions are almost identical for deposits on RVC (solid line in Fig. 1) and Au wires (dotted line). Fig. 3 also demonstrates that for the Pd–Rh/RVC system the hysteresis is smaller than for Pd/RVC. Similar behavior was observed for thin deposits on Au wires [14]. The effect of hysteresis is important in the context of energy storage since it is one of the factors determining energy loss in a charging/discharging cycle of hydride batteries [15]. Thus, reducing hysteresis increases the energetic efficiency of the system as an electrochemical power source. Another feature of the data shown in Fig. 3 is slightly lower potential of the α–β phase transition for the alloy in comparison with pure Pd. It is the effect of a smaller lattice parameter of Pd–Rh alloys with respect to Pd (so-called 'contracted alloys') [5,6]. Such behavior is a consequence of an additional work to be done to extend the lattice in a contracted system during the α–β transition [8].

Fig. 4 presents the potential dependence of the time needed to obtain a steady-state electrode saturation with hydrogen and the time necessary for hydrogen oxidation, determined from chronoamperometric curves (Fig. 5). It demonstrates that with a decrease in the electrode potential (and a simultaneous increase

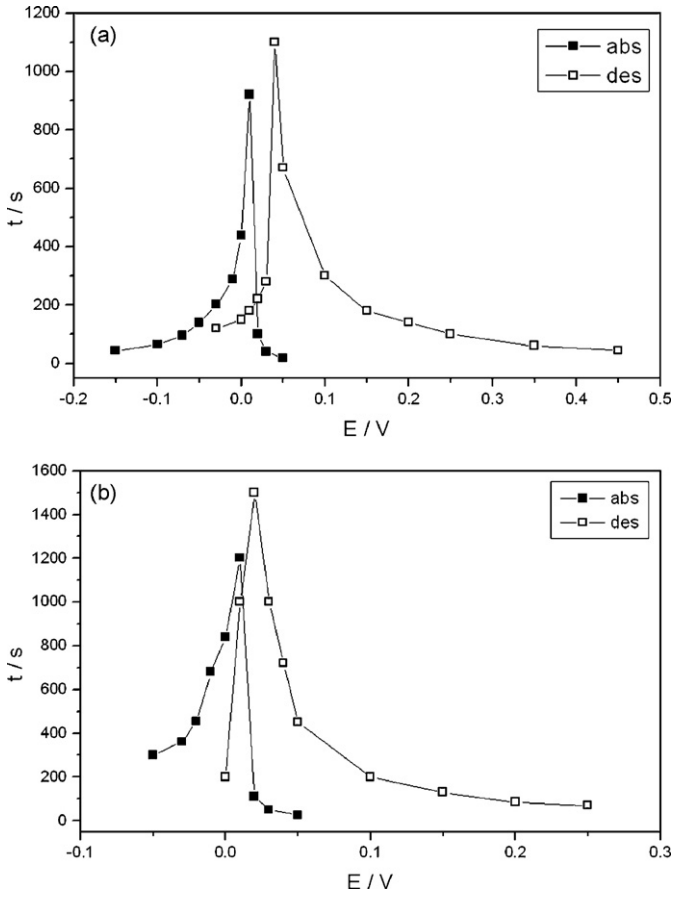


**Fig. 4.** Time needed for a steady-state saturation of the electrode with hydrogen (solid symbols) and time needed for the oxidation of hydrogen electrosorbed at −0.05 V (open symbols) in 0.5 M $H_2SO_4$ vs. potential of absorption and desorption, respectively: (a) Pd/RVC, (b) 97% Pd–Rh/RVC.

in the amount of absorbed hydrogen) the absorption time initially slowly increases, then passes through a sharp maximum and finally gradually decreases. Analogous dependence has been found for increasing potential of hydrogen desorption, but with the maximum placed at a slightly higher potential.

The existence of a maximum on the *t*–*E* dependence indicates the potential where the rate of the absorption/desorption process reaches the minimum value. Such behavior has also been observed for thin layers of Pd and its alloys deposited on Au wires [14,50,53,54]. The only difference was that for RVC electrodes the respective time values are higher than for Au wires. This, however, can be explained by larger total volume of hydrogen-absorbing material in the former case.

A comparison of the potentials of time maxima with the respective H/Pd–*E* or H/(Pd + Rh)–*E* plots for absorption and desorption reveals that these potentials are always within the phase transition region. Moreover, the maximum absorption time corresponds to the highest potential sufficient for β-phase formation and the maximum desorption time is connected with the lowest potential sufficient for β-phase decomposition. Thus, we can conclude that the slow process of α–β transition rather than surface kinetics or bulk diffusion controls the overall rate of hydrogen absorption and desorption into/from thin Pd-based layers [55–57]. The low rate of phase transition is also mirrored in the courses of both absorption and desorption chronoamperograms with inflexion points present at the initial parts of *i*–*t* curves (indicated by arrows in Fig. 5), where a rapid decrease in the current (see region A in the inset in Fig. 5) is followed by a region of a lower slope or even a plateau (region B). It has been found that for an absorption step the charges passed up to those points correspond to the amounts of hydrogen only slightly higher than its maximum concentration in the α-phase. On the other hand, in the case of a desorption step the charges consumed before the inflexion points (area C) are very close to the differences between the total amount of absorbed hydrogen and its minimum concentration in the β-phase. Thus, the characteristic points on *i*–*t* curves indicate the onset of the β-phase formation or decomposition, respectively.

Fig. 6 shows open circuit potential measured after sample saturation with hydrogen at −0.03 V. A long period of almost constant potential (ca. 0.01–0.03 V) is observed corresponding to β- and α-phase coexistence, followed by rapid increase up to ca. 0.7–0.8 V, i.e. a value at which no form of hydrogen is present in Pd or the Pd–Rh alloy. These data demonstrate that in the absence of external hydrogen the Pd–hydrogen system is unstable and its spontaneous dehydriding occurs. According to the literature [58,59] hydrogen absorbed in Pd has a tendency to leave the metal, since without

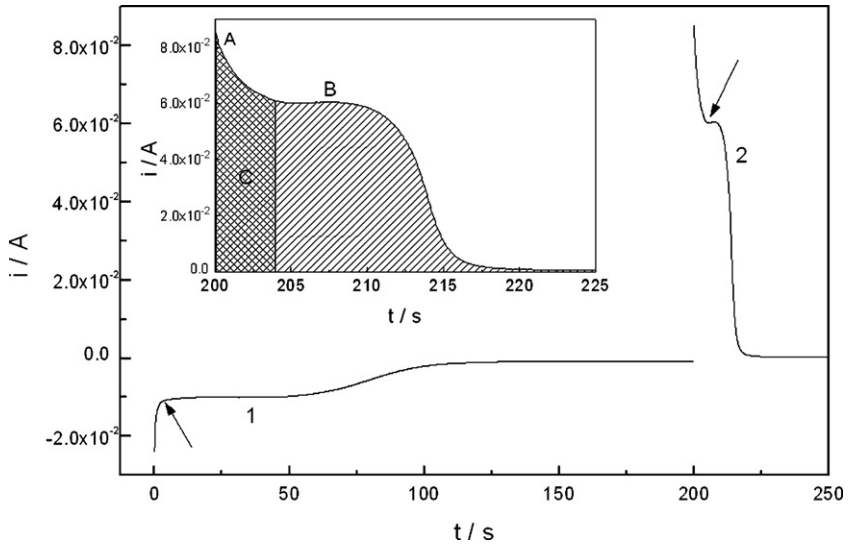


**Fig. 5.** Chronoamperograms recorded for Pd/RVC in 0.5 M $H_2SO_4$ according to potential program: pretreatment at 0.45 V, cathodic step (1) hydrogen electrosorption at −0.05 V, anodic step (2) hydrogen oxidation at 0.45 V.

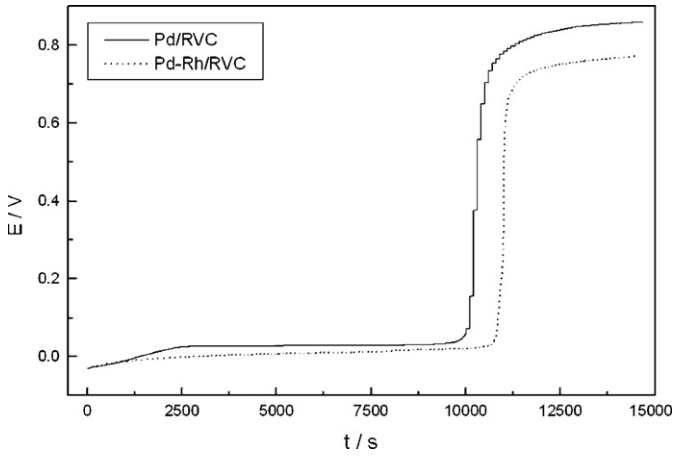


**Fig. 6.** Open circuit potential vs. time after hydrogen absorption (1200 s at −0.03 V) in: (a) Pd/RVC and (b) 97% Pd–Rh/RVC.

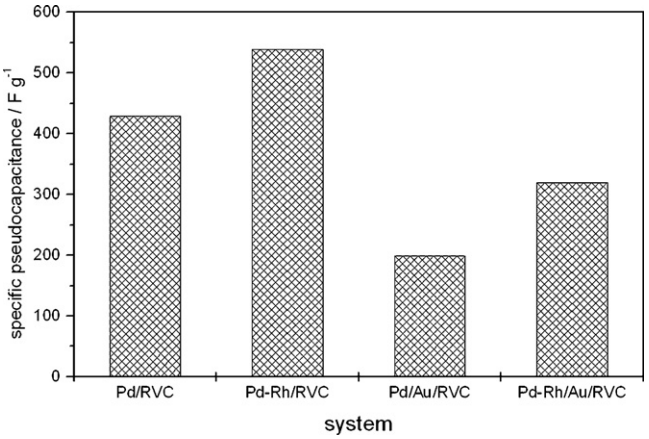


**Fig. 7.** Maximum values of specific pseudocapacitance obtained for voltammetric (0.005 V $s^{-1}$) oxidation of hydrogen absorbed in Pd and Pd–Rh alloys deposited on RVC.

hydrogen in the solution the Pd–H equilibrium is strongly shifted towards hydrogen desorption.

The presence of potential plateau in Fig. 6 can be explained by Gibbs phase rule—as long as β and α-phases coexist, electrode potential is independent of the state of charging with hydrogen. One should note lower potential of the plateau for the Pd–Rh alloy than for Pd, which results from the aforementioned lattice contraction of the alloy. However, once the β-phase decomposition is completed, only one phase is present in the system and potential can change, eventually reaching the values corresponding to surface oxidation of the electrode. Lower final potential for the Pd–Rh alloy is in line with the fact that Rh addition to Pd makes the electrode surface easier for oxidation [60].

The analysis of the above data confirms earlier statements [19,20,38] that there is no qualitative influence of RVC substrate on the absorption behavior of Pd-based deposits. The main differences concern timescale of the processes, which can result from specific geometry of RVC material. Another feature, which is manifested on CV curves at high scan rates, is an uncompensated IR drop inside the pores of RVC. There are also considerably higher double layer charging currents due to the highly developed electrode surface [38]. However, when stationary measurements are performed during a period long enough to obtain equilibrium conditions, the results for RVC electrodes are in agreement with the data reported for thin Pd-based layers deposited on other substrates [14,16–20]. This statement is also true for the comparison between the deposits on bare RVC and RVC first electroplated with Au [38]. The latter kind of matrix, however, allows for better deposit adhesion to the substrate during repeated hydrogen absorption/desorption runs.

The amount of hydrogen absorbed in Pd-based materials can be recalculated into units commonly used for description of energy storage systems, i.e. pseudocapacitance per mass unit. This was done on the basis of the ratio between charge of absorbed hydrogen oxidation and the potential range in which all absorbed hydrogen is electrochemically removed during an anodic CV scan [61]. Pseudocapacitance characteristics referred to the total mass (i.e. the sum of deposit and substrate masses) of Pd and Pd–Rh hydrogen absorbers deposited on RVC are shown in Fig. 7. The maximum values of specific pseudocapacitance reach more than 500 F $g^{-1}$, i.e. are comparable with the data reported for supercapacitors based on reversible insertion of atomic species into the crystal structure of bulk solid electrodes, e.g. polymers or $RuO_2$ [25], and higher than the values typical of double layer electrochemical capacitors [26]. It should be stressed that specific capacitance of bare RVC under the same experimental condition did not exceed 0.1 F $g^{-1}$, i.e. was negligible in comparison with psedocapacitance originating from redox processes of hydrogen absorption/desorption (see also CV curves in Fig. 2).

The values of specific power are collected in Fig. 8. They were calculated in various ways, both for chronoamperometric and voltammetric oxidation of hydrogen absorbed at −0.05 V. In the former case average power (CAav) was obtained as the product of charge-to-time ratio during total removal of absorbed hydrogen and the difference between potentials corresponding to hydrogen absorption (−0.05 V) and oxidation (0.45), while in the latter case (CVav) it was obtained as the product of scan rate applied (here 0.005 V $s^{-1}$) and charge consumed during hydrogen oxidation [61]. Additionally, the values of specific power were calculated for maximum (CAmax – for region A in Fig. 5) and plateau (CAplat – region B) current in chronoamperometric oxidation as well as for peak current (CVp) in voltammetric oxidation. All these values are in the range 0.5–6.0 W $g^{-1}$, i.e. of the same order of magnitude as the characteristics of typical supercapacitors [61–65]. Moreover, maximum values of specific energy exceeded 20 Wh $kg^{-1}$, again within the range reported in the literature for this class of systems [62,64].

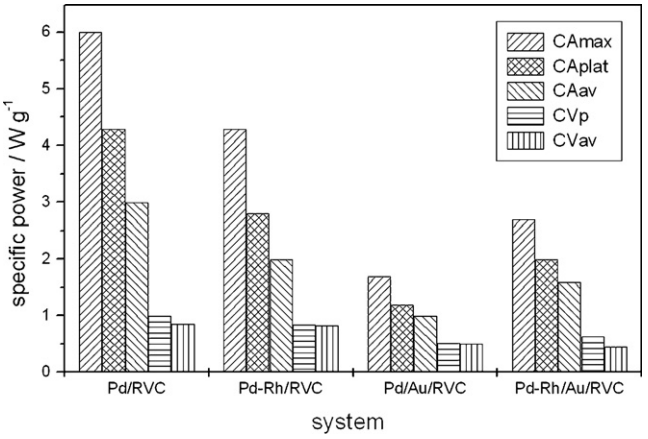


**Fig. 8.** Maximum values of specific power obtained for oxidation of hydrogen absorbed at −0.05 V in Pd and Pd–Rh alloys deposited on RVC: CAmax, specific power corresponding to maximum current in chronoamperometric oxidation (0.45 V); CAplat, specific power corresponding to current plateau in chronoamperometric oxidation (0.45 V); CAav, average specific power in chronoamperometric oxidation (0.45 V); CVp, specific power corresponding to current peak in voltammetric oxidation (0.005 V $s^{-1}$); CVav, average specific power in voltammetric oxidation (0.005 V $s^{-1}$).

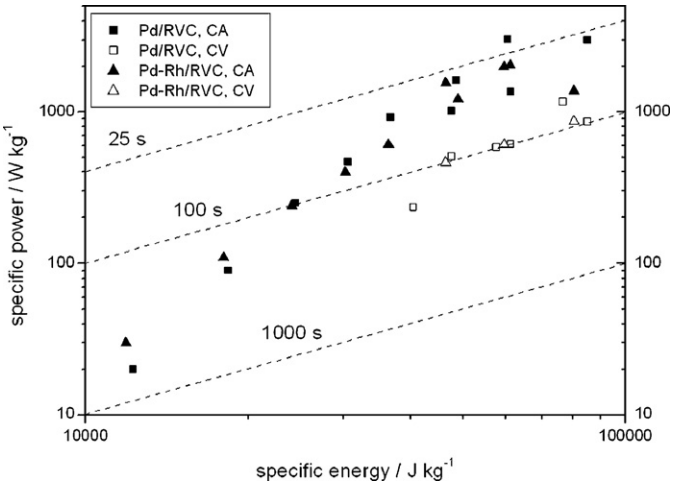


**Fig. 9.** Ragone plot for chronoamperometric (CA) and voltammetric (CV) oxidation of hydrogen absorbed in Pd and Pd–Rh alloys deposited on RVC. Dotted lines correspond to various discharging times.

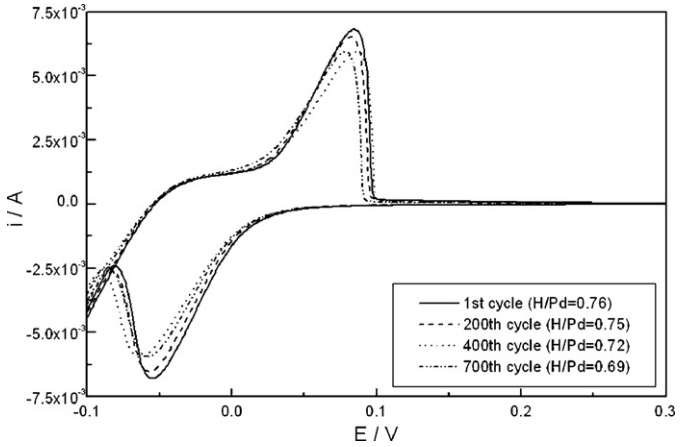


**Fig. 10.** Cyclic voltammograms (0.001 V $s^{-1}$) for Pd/Au/RVC electrode subjected to continuous potential cycling in 0.5 M $H_2SO_4$. H/Pd ratios shown in the legend.

It would be interesting to compare the parameters of Pd-based/RVC supercapacitors with other type of devices utilizing hydrogen absorption in metals/alloys, i.e. nickel-hydride batteries (Ni-MH). The latter systems are characterized by higher specific energy (55–70 Wh $kg^{-1}$) [15] but lower specific power (typically below 1 W $g^{-1}$) [65] than our system studied. It should be added that hydrogen diffusion coefficient in metal hydrides used in most commercially available batteries is at least two orders of magnitude lower than in Pd–H system ($10^{-8}$ to $10^{-10}$ vs. $10^{-6}$ to $10^{-7}$, respectively) [1,15], thus higher diffusional limitations are expected in the case of Ni-MH. It should be added that since capacitance of the Pd–H system is essentially based on pseudocapacitance resulting from redox processes occurring in the bulk of electroactive material, this type of supercapacitor is somewhat battery-like in its behavior [63].

The latter fact is confirmed by the course of Ragone plot (i.e. specific power vs. specific energy) for Pd-based/RVC supercapacitors (Fig. 9). In contrast to the case of double layer capacitors, in which the increase in specific energy results in a decrease in specific power [65,66], our systems studied exhibit the increase in power with energy. This effect was predicted by Pell and Conway [66] for batteries and supercapacitors based on faradaic pseudocapacitance under the conditions of sufficiently high discharge currents, i.e. corresponding to the energy region before the maximum power is reached. This maximum is visible in Fig. 9 at the right-hand side of Ragone plot. Thus, it can be concluded that the systems examined may operate at both high energy and power. It should be noted that during discharging of hydrogen-saturated Pd or Pd–Rh alloys the potential remains practically constant as long as β and α phases coexist (see Fig. 6). This is another similarity to battery-like behavior, as for a typical capacitor the potential decline with the extent of discharge is observed [66].

Although one can recognize the slow α–β phase transition in Pd-based systems as their main disadvantage that limits the rate of charging–discharging processes, it should be stressed that relatively high currents can still be achieved during dehydriding of pure β-phase (region A in the inset in Fig. 5). In fact, the values of hydrogen loading/deloading time at extreme charging and discharging potentials (−0.05 and 0.45 V, respectively) are of the order of minutes being comparable with literature data for supercapacitors based on carbon, polymers or metal oxides [61–63]. Moreover, kinetic parameters might be improved by applying thinner layers than used in our study. Also, it is possible the absorption–desorption hysteresis to be decreased by higher Pd substitution with Rh without significant deterioration of hydrogen absorption capacity (up to 20% Rh in the alloy bulk the amount of absorbed hydrogen is higher than in pure Pd [14]).

Fig. 8 also demonstrates that the values of average specific power calculated for voltammetric oxidation are lower than under potentiostatic conditions. This difference mirrors the fact that for polarization between −0.05 and 0.45 V at scan rate 0.005 V $s^{-1}$ time needed for the oxidation of all absorbed hydrogen is higher than during polarization at constant potential of 0.45 V, therefore charge consumed in time unit is lower. Also, in Figs. 7 and 8 it is visible that in the case of Pd and Pd–Rh deposits on RVC electroplated with Au the values of specific pseudocapacitance and power are lower than for the deposits on bare RVC. However, the use of Au as an intermediate layer between Pd-based deposit and RVC matrix seems to be more appropriate for real applications due to better deposit adhesion to the substrate [38,67,68].

Fig. 10 shows hydrogen absorption–desorption currents recorded for Pd/Au/RVC electrode during continuous potential cycling. This procedure was applied to check charging–discharging durability of a potential supercapacitor. No significant deterioration of hydrogen absorption capacity was observed even after 700 cycles, i.e. the changes in H/Pd ratio did not exceed 10%. However, further cycling led to some loss in hydrogen absorption capacity due to partial dropping off the coating after repeated hydrogen insertion and removal, which is connected with crystal lattice expansion/contraction accompanying α–β and β–α phase transitions [5,6]. It should be stressed that the cycle-ability of the Pd/Au/RVC system was much better than that of Pd deposited on bare RVC. In the latter case already after 200 cycles the deposit adhesion became weaker and H/Pd ratio decreased.

Comparing Fig. 10 with Fig. 2 one should note some differences in the hydrogen absorption/desorption currents. In Fig. 10 a pair of peaks is observed (cathodic at ca. −0.06 V and anodic at ca. 0.08 V), while in Fig. 2 the large cathodic peak is not present; instead a small wave at ca. 0.17 V is visible. The differences between both CV curves originate from different scan rates applied. Fig. 2 corresponds to higher scan rate (0.01 V $s^{-1}$) than Fig. 10 (0.001 V $s^{-1}$). Since hydrogen absorption is relatively slow, during faster polarization not all available amount of hydrogen can be absorbed and the cathodic peak in not developed. At higher scan rate hydrogen adsorption peak (i.e. the aforementioned signal at 0.17 V) is much more pronounced, since the contribution of the bulk process of hydrogen absorption to the overall hydrogen signal is smaller. The differences in signal shape and potential may also be partially due to IR drop effect that occurs as a result of RVC porosity. This effect is expected

to increase with scan rate. However, the separation between anodic and cathodic hydrogen peaks observed even at low scan rate indicates a certain degree of electrochemical irreversibility of hydrogen absorption and desorption. As was discussed in detail in our earlier works [14,50], this behavior originates from a slow α–β phase transition.

Therefore, in that context it would be interesting to investigate a hydrogen–metal system which is homogeneous, i.e. where single phase exists during hydrogen loading and therefore no phase transition occurs. However, for the use in supercapacitors the amount of absorbed hydrogen in that phase should be distinctly higher than in the α-phase in pure Pd. Such features are exhibited by Pd alloys with Au or Ag containing ca. 20–30% of solute metal [1,5,6]. Moreover, these alloys exhibit faster kinetics of hydrogen absorption/desorption [69,70]. Thus, further research is needed to examine these systems in the aspect of possible applications in supercapacitors.

## 4. Conclusions

Pd and Pd–Rh alloys can be potentiostatically deposited on RVC matrix. Such electrodes exhibit electrochemical properties typical of the deposits, not influenced qualitatively by RVC substrate. The slow processes of phase transitions control the rate of hydrogen absorption and desorption into/from thin Pd-based/RVC layers. Under open circuit conditions spontaneous decomposition of the β-phase occurs and electrode potential is determined by α–β phase equilibrium. The values of specific pseudocapacitance, specific power and specific energy calculated for the process of hydrogen oxidative desorption from Pd and Pd–Rh alloys deposited on RVC are comparable with those typical of supercapacitors utilizing various redox reactions. Further studies are certainly needed to solve several problems before these systems find their real applications.

## Acknowledgements

The research was financed within a framework of 6FP HydroNanoPol project and a SPB HydroNanoPol project financially supported by Ministry of Science and Higher Education (MNiSW).

## References

[1] F.A. Lewis, The Palladium/Hydrogen System, Academic Press, New York, 1967.
[2] G. Jerkiewicz, Prog. Surf. Sci. 57 (1998) 137.
[3] T.B. Flanagan, Y. Sakamoto, Plat. Met. Rev. 37 (1993) 26.
[4] F.A. Lewis, Plat. Met. Rev. 5 (1961) 21.
[5] Y. Sakamoto, K. Baba, T.B. Flanagan, Z. Phys. Chem. N. F. 158 (1988) 223.
[6] Y. Sakamoto, K. Yuwasa, K. Hirayama, J. Less-Common Met. 88 (1982) 115.
[7] F.A. Lewis, Plat. Met. Rev. 4 (1960) 132.
[8] E. Wicke, K. Frölich, Z. Phys. Chem. N. F. 163 (1989) 35.
[9] K. Kandasamy, F.A. Lewis, W.D. McFall, R.-A. McNicholl, Z. Phys. Chem. N. F. 163 (1989) 41.
[10] Y. Sakamoto, F.L. Chen, M. Ura, T.B. Flanagan, Ber. Bunsenges. Phys. Chem. 99 (1995) 807.
[11] R. Burch, Trans. Faraday Soc. 66 (1970) 736.
[12] N. Comisso, A. De Ninno, E. Del Giudice, G. Mengoli, P. Soldan, Electrochim. Acta 49 (2004) 1379.
[13] Y. Sakamoto, Y. Haraguchi, M. Ura, F.L. Chen, Ber. Bunsenges Phys. Chem. 98 (1994) 964.
[14] A. Żurowski, M. Łukaszewski, A. Czerwiński, Electrochim. Acta 51 (2006) 3112.
[15] J. Kleperis, G. Wójcik, A. Czerwiński, J. Skowroński, M. Kopczyk, M. Bełtowska-Brzezińska, J. Solid State Electrochem. 5 (2001) 229.
[16] A. Czerwiński, I. Kiersztyn, M. Grdeń, J. Czapla, J. Electroanal. Chem. 471 (1999) 190.
[17] A. Czerwiński, I. Kiersztyn, M. Grdeń, J. Electroanal. Chem. 492 (2000) 128.
[18] A. Czerwiński, I. Kiersztyn, M. Grdeń, J. Solid State Electrochem. 7 (2003) 321.
[19] A. Czerwiński, R. Marassi, S. Zamponi, J. Electroanal. Chem. 316 (1991) 211.
[20] A. Czerwiński, Polish J. Chem. 69 (1995) 699.
[21] A. Czerwiński, J. Electroanal. Chem. 379 (1994) 487.
[22] A. Czerwiński, S. Zamponi, R. Marassi, J. Electroanal. Chem. 304 (1991) 233.
[23] A. Czerwiński, M. Grdeń, M. Łukaszewski, J. Solid State Electrochem. 8 (2004) 411.
[24] M. Łukaszewski, M. Grdeń, A. Czerwiński, J. Phys. Chem. Solids 65 (2004) 523.
[25] R.A. Huggins, Solid State Ionics 134 (2000) 179.
[26] E. Frąckowiak, F. Béguin, Carbon 39 (2001) 937.
[27] B.E. Conway, J. Electrochem. Soc. 138 (1991) 1539.
[28] S. Sarangapani, B.V. Tilak, C.-P. Chen, J. Electrochem. Soc. 143 (1996) 3791.
[29] J. Wang, Electrochim. Acta 26 (1981) 1721.
[30] J.M. Friedrich, C. Ponce-de-León, G.W. Reade, F.C. Walsh, J. Electroanal. Chem. 561 (2004) 203.
[31] Z. Rogulski, W. Lewdorowicz, W. Tokarz, A. Czerwiński, Polish J. Chem. 78 (2004) 1357.
[32] S. Zamponi, M. Dimarino, R. Marassi, A. Czerwiński, J. Electroanal. Chem. 248 (1988) 341.
[33] S. Zamponi, A. Czerwiński, R. Marassi, J. Electroanal. Chem. 266 (1989) 37.
[34] A. Czerwiński, J. Sobkowski, R. Marassi, Anal. Lett. 18 (A14) (1985) 1717.
[35] A. Czerwiński, R. Marassi, J. Sobkowski, Ann. Chim. 74 (1984) 681.
[36] A. Frydrychewicz, A. Czerwiński, K. Jackowska, Synth. Met. 121 (2001) 1401.
[37] A. Frydrychewicz, S.Y. Vassiliev, G.A. Tsirlina, K. Jackowska, Electrochim. Acta 50 (2005) 1885.
[38] A. Czerwiński, M. Łukaszewski, A. Żurowski, H. Siwek, S. Obrębowski, J. New Mater. Elect. Syst. 9 (2006) 419.
[39] A. Czerwiński, Anal. Lett. 20 (4) (1987) 503.
[40] A. Czerwiński, M. Dmochowska, M. Grdeń, M. Kopczyk, G. Wójcik, G. Młynarek, J. Kołata, J.M. Skowroński, J. Power Sources 77 (1999) 28.
[41] A. Czerwiński, M. Żelazowska, J. Electroanal. Chem. 410 (1996) 55.
[42] A. Czerwiński, M. Żelazowska, J. Power Sources 64 (1997) 29.
[43] Z. Rogulski, A. Czerwiński, J. Power Sources 114 (2003) 176.
[44] Z. Rogulski, A. Czerwiński, J. Solid State Electrochem. 7 (2003) 118.
[45] Z. Rogulski, M. Chotkowski, A. Czerwiński, J. New Mater. Elect. Syst. 9 (2006) 333.
[46] D. Pletcher, R. Wills, Phys. Chem. Chem. Phys. 6 (2004) 1779.
[47] E. Gyenge, J. Jung, B. Mahato, J. Power Sources 113 (2003) 388.
[48] E. Gyenge, J. Jung, S. Splinter, A. Snaper, J. Appl. Electrochem. 32 (2002) 287.
[49] M. Łukaszewski, A. Żurowski, M. Grdeń, A. Czerwiński, Electrochem. Commun. 9 (2007) 671.
[50] M. Łukaszewski, M. Grdeń, A. Czerwiński, J. Electroanal. Chem. 573 (2004) 87.
[51] T.B. Flanagan, C.-N. Park, W.A. Oates, Prog. Solid State Chem. 23 (1995) 291.
[52] D. Wang, T.B. Flanagan, T. Kuji, Phys. Chem. Chem. Phys. 4 (2002) 4244.
[53] M. Grdeń, A. Piaścik, Z. Koczorowski, A. Czerwiński, J. Electroanal. Chem. 532 (2002) 35.
[54] M. Grdeń, K. Kuśmierczyk, A. Czerwiński, J. Solid State Electrochem. 7 (2002) 43.
[55] W.-S. Zhang, X.-W. Zhang, X.-G. Zhao, J. Electroanal. Chem. 458 (1998) 107.
[56] P. Millet, M. Srour, R. Faure, R. Durand, Electrochem. Commun. 3 (2001) 478.
[57] P.A. Bennett, J.C. Fuggle, Phys. Rev. B 26 (1982) 6030.
[58] S. Schuldiner, G.W. Castellan, J.P. Hoare, J. Chem. Phys. 28 (1958) 16.
[59] J.M. Rosamilia, J.A. Abys, B. Miller, Electrochim. Acta 36 (1991) 1203.
[60] M. Łukaszewski, A. Czerwiński, J. Solid State Electrochem. 11 (2007) 339.
[61] T. Cottineau, M. Toupin, T. Delahaye, T. Brousse, D. Bélanger, Appl. Phys. A 82 (2006) 599.
[62] C. Arbizzani, M. Mastragostino, F. Soavi, J. Power Sources 100 (2001) 164.
[63] A.G. Pandolfo, A.F. Hollenkamp, J. Power Sources 157 (2006) 11.
[64] E. Faggioli, P. Rena, V. Danel, X. Andrieu, R. Mallant, H. Kahlen, J. Power Sources 84 (1999) 261.
[65] M. Mastragostino, F. Soavi, J. Power Sources 174 (2007) 89.
[66] W.G. Pell, B.E. Conway, J. Power Sources 63 (1996) 255.
[67] A. Czerwiński, A. Żurowski, M. Łukaszewski, Patent Pending P-375062, 2005 (Poland).
[68] A. Czerwiński, Przem. Chem. 85 (2006) 1186.
[69] M. Łukaszewski, A. Czerwiński, J. Solid State Electrochem 12 (2008) 1589.
[70] S.-Y. Liu, Y.-H. Kao, Y. Oliver Su, T.-P. Perng, J. Alloys Compd. 293–295 (1999) 468.